International Journal of Thin Films Science and Technology

http://dx.doi.org/10.18576/ijtfst/120208

Effect of RF Sputtered on Characterization of SrTiO3 Thin Film

Hamed A. Gatea[1,*], *Hashim Abbas*[2], *and Saja hameed kareem*[3]

[1]Department of Medical Physics, Al-Mustaqbal University College 51001, Hillah, Babylon, Iraq
[2]Department of Optics, Collage of Health and Medical Technology, Al-Ayen University, Thi-Qar, Iraq
[3]Collage of Pharmacy, National University of Science and Technology, Dhi Qar, Iraq

Received: 2 Feb. 2023, Revised: 3 Mar. 2023, Accepted: 22 Apr. 2023
Published online: 1 May 2023

Abstract: Thin films of SrTiO3 (STO) were formed on p-type Si(100) substrates using rf magnetron sputtering at different substrate temperatures. The structural and electrical properties were investigated. The thickness of the films was between 300 and 500 nm, and the substrate temperature was always 550°C. The XRD pattern shows the cubic phase for SrTiO3 thin film. Using capacitance-voltage, current-voltage, and admittance spectroscopy, metal-insulator-semiconductor (Al/STO/p-Si/Al) structures were fabricated and characterized. The dielectric constant decreased with increasing frequency. The impedance decreased with increasing frequency.

Keywords: SrTiO3 film, Electrical properties, Ferroelectric materials, Perovskite structure.

1 Introduction

SrTiO3 is ferroelectric materials that has para-electric phase. A ferroelectric material is one which can, or can be realistically conceived to undergo one or more ferroelectric phase transitions [1,2]. “The ferroelectric materials have salient features such as a spontaneous polarization component which can be reversed by the application of strong enough electric field and the spontaneous – polarization vector of a ferroelectric specimen has at least one component which is a non-linear and double-valued function of electric field” [1,2,3,4,5]. The hysteresis thus observed is a function of the work required to displace the domain walls and is closely related to both the detect distribution in the crystalline to the energy barrier separating the different orientation state [6,7]. At room temperature, SrTiO3 crystallizes in the ABO3 cubic perovskite structure (space group Pm3m) with a lattice parameter of 0.3905 nm and a density of = 5.12 g / cm^3 [2,8]. Strontium Titanate, or SrTiO3, is a single crystal that has an excellent lattice match to most Perovskite materials[5,9]. It exists in the cubic form at ambient temperature but changes to the tetragonal structure at temperatures below 105K [10,11]. SrTiO3 appears superconducting and piezoelectric properties at very low temperatures. Additionally, it has a relatively high dielectric constant [12,13].

“SrTiO3 in the perovskite structure is a very attractive material for application to microelectronics because of its high charge storage capacity, good insulating properties and excellent optical transparency in the visible region and chemical stability [14,15]. In the past, due to lattice parameter match, SrTiO3 was largely employed as substrate for epitaxial growth of high temperature superconducting films [16,17]”. SrTiO3 has also attracted a great deal of interest in the world of oxide electronics, not only as a high dielectric constant insulator, but also as a wide-gap semiconductor with a band gap of 3.2 eV [18]. Conductivity is more accurately controlled by doping than oxygen deficiency control. The ability to control conductivity in SrTiO3 is important in the design of various electro ceramic devices such as capacitors, metal oxide semiconductor field effect transistors (MOSFET’s), thermostats and varsities. This work investigated properties of SrTiO3 film prepared by RF sputtering, the structure, dielectric properties and conductivity studied in this paper.

*Corresponding author E-mail: hamedalwan14@gmail.com

Table 1. Describe of properties of SrTiO3

"Physical Properties"	
"Crystal Structure"	"Cube a=3.905A"
"Growth Method"	"Flare"
"Density"	"5.175g/cm^3 "
"Melt point "	"2080°C"
"Hardness"	"6Mohn"
"Thermal expansion"	"10.4×10-6/°C2
"Dielectric constant"	"300"
"Zoss Tangent at 10GHZ"	"5×10-4@300k 3×10-4@>>k"
"Color and Appearance"	"Light brown under the light"
"Chemical stability"	"Undissolvable in water"

2 Experimental Methods

The selection of starting materials, the procedure adopted for processing of materials and the synthesis route determine the quality of the end product. The quality and physical behaviour of the final phase depends on the synthesis method adopted. The performance characteristics depend on the repeatability of the physical properties of the material. There are quite a good number of ways to prepare materials in ceramic form: (a) Solid state reaction method,(b) Sol-Gel method, (c) Hydrothermal synthesis, (d) Co-precipitation method.The raw materials are normally carbonates or nitrates of the constituents. Impurities and particle size affects the reactivity as well as the properties of the finished product like compressibility, shrinkage, conductive properties of the materials. Chemicals used for preparation of the samples in the present work are all Sigma-Aldrich make and their purity is about more than 99 %. The stoichiometric amounts of nitrate powders were dissolved in double distilled water, all in the correct molar proportions. The individual solutions were combined, and an aqueous citric acid solution proportional to each mole of metal atom was added. All of the metals in the mix had to be bind by the amount of citric acid that was used. It is crucial to note that the pH of the solution must be lower than 7, as higher pH values will cause the formation of hydroxides and basic salts. The solution was slowly heated over a temperature controlled hot plate until a viscous mass was obtained.

Ethylene glycol was added and heated over the temperature 160-1800C to get the gel. Then there was a big growth, and then the reaction started, and a fine, uniform powder was made. "The powders were calcined at 6000C- for 5 hours in air. The calcined powders were ground and pressed into pellets. The pellets were finally sintered at the temperature 11000C-13000C for 4 hours. The flow chart of preparation of samples is shown in Fig. 1."

In the present study, cylindrical pellets of 2 inch diameter and 1-2 mm thick samples were compacted using Khosala make hydraulic press at a pressure of 1-2 MPa. This is due

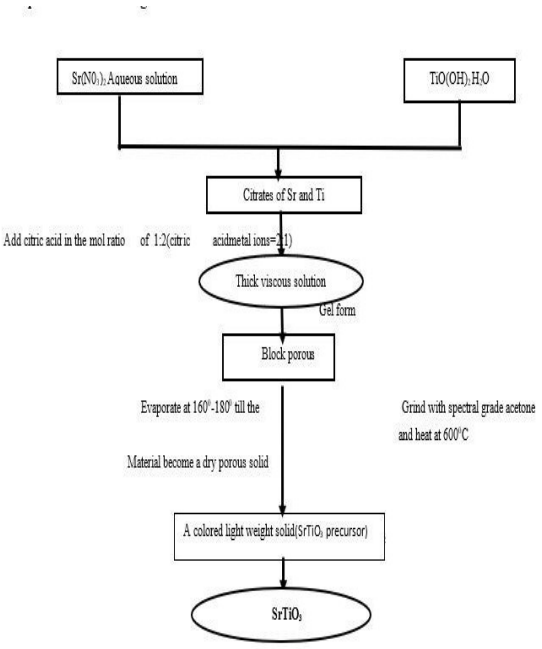

Fig. 1: flow chart prepared SrTiO3 film.

to reduction of the total surface area by an increase in the average grain size of the particle, reduction of pores, which leads to densification.

Radiofrequency (RF) sputtering is a technique used to produce thin films used in the computer and semiconductor industries. These ions strike the target material, which will eventually form the thin film coating, and break it up into a fine spray that covers the substrate, which will serve as the thin film's inner foundation. The voltage, system pressure, sputter deposition pattern, and optimal target material for RF

Sputtering are different from those for D.C. sputtering. The target material, substrate, and RF electrodes commence the RF sputtering process in a vacuum chamber. The inert gas, which is commonly argon, neon, or krypton depending on the size of the molecules in the target substance, is then delivered into the chamber.

The radio waves are then used to ionize the gas atoms in the plasma by turning on the RF power source. Once the ions start to hit the target material, it breaks up into small pieces that move to the substrate and start to form a layer. The inert gas plasma in an RF system can be maintained at less than 15 mTorr, compared to 100 mTorr for DC sputtering, due to the difference powering mechanism.

3 Theoretical parts:

The electrical conductivity is defined as

$\sigma = 1/\rho$ ----------(1)

"where is the ρ resistivity of the material. If R is resistance of the sample of thickness t and cross sectional area A", the electrical conductivity is given by

$\sigma = t/RA$ ----------(2)

The DC conductivity was calculated using the equation 2.6. A graph is plotted between

"log(σ) and 1000/T to evaluate the activation energies. The following Arrhenius equation is used to evaluate the activation energies".

$\sigma = \sigma_o e^{-E/kT}$ ----------(3)

"where 'E' is the activation energy (in eV), 'k' the Boltzman's constant and 'T' the absolute temperature".

The behavior of a material within a parallel plate capacitor can define its dielectric properties. When two plates of the same area are separated in free space by a little distance, then the capacitance of the capacitor is

$$C_0 = \frac{\varepsilon_0 A}{t}$$ ----------(4)

"Where ε0 is the permittivity of the free space, 'A' is the area of the plate and 't' is the distance between the plates". If you put an insulating material between the plates of a parallel plate capacitor, the capacitor's capacitance goes up.

The impedance is a complex parameter and it contains real (Z') and imaginary (Z'') terms. The complex impedance is represented as,

$Z^* = Z' - jZ''$ ----------(5)

Its magnitude is ."The real and imaginary parts of the complex impedance are given by",

$Z' = Z\cos(\theta)$ and $Z'' = Z\sin(\theta)$ with the phase angle $\theta = \tan^{-1}(Z''/Z')$

Impedance measurements were performed as a function of frequency and temperature using Autolab (PGSTAT 30) low frequency impedance analyzer interfaced to a PC. The results were analyzed using frequency response analyser (FRA) software.

"The complex impedance of the RC combination if a resistance (R) and a capacitance (C) are linked in parallel is given by"[7],

$$\frac{1}{Z^*} = Y^* = \left(\frac{1}{R} + \frac{1}{j\omega C}\right)$$ ----------(6)

"where Y* is the complex admittance which also contains real and imaginary terms i.e".,

$Y^* = Y' + jY''$ ----------(7)

The variation of imaginary part of impedance with frequency at different temperatures was studied to observe the relaxation processes and also to know the effect of space charges in the material. The variation of real and imaginary parts of impedance are given by,

The admittance (Y) is a way to measure how easy it is for a current to run through a circuit or device. It is defined as the impedance inverse (/). The Siemens is the SI unit of admittance. (symbol S)

$Y' = Z^{-1} = 1/Z$ ----------(8)

"Where, Y is the admittance, measured in Siemens, Z is the impedance, measured in ohms"

"Ohm's law of circuit theory states that the resistance of a material is equal to the applied voltage divided by the current drawn across the material between two electrodes"[4].

$R = V/I$ ----------(9)

"Where, R=Resistance (ohms), V= Voltage (volts), I = Current (amperes, A)"

This electrical resistance is related to the length and resistivity of the sample and is oppositely related to the sample's cross-sectional area.

$R = \rho\, l/A$ ----------(10)

"Where, ρ = Resistivity, A =cross- sectional area, l = length"

Ohms are the physical unit for surface resistance. Surface resistivity is frequently expressed in Ω/square units in practice. This unit should be considered a logo rather than a physical unit of surface resistivity. Despite this, it is essential to comprehend the meaning of Ω /square because

it is the unit of surface resistivity in the majority of published works.
Then, equation 2 could be written as,

$\rho = R\ wt/l = Rw/l$----------(11),

Where, w = width, l = length

4 Results and Discussion

4.1 X-ray diffraction (XRD)

The crystalline phases of the specimen are determined by this diffraction pattern, and its structural characteristics are calculated. Consequently, Scherrer's formula may yield results that differ from the actual particle sizes. Although the estimation would only work for extremely small particles, this technique is quite effective in characterizing SrTiO3 films. XRD can also be used to estimate the film thickness of epitaxial and highly textured thin films. Figure 2 shows the powder XRD spectra of a series of SrTiO3 film."X-ray diffraction (XRD) studies were carried out to show the crystallinity using X-ray diffractometer with CuKα radiation (λ=1.54406 oA); (the range of 2θ was (20-80o))".

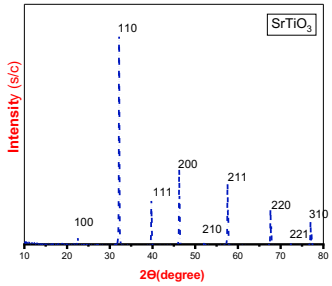

Fig. 2: XRD pattern of SrTiO3 thin films prepared by RF sputtering.

4.2 Dielectric properties:

The electrical properties of polycrystalline SrTiO3 on p-type Si(100) substrates These properties include the d.c conductivity, A.C behavior, the C-V characteristics measurements of the (SrTiO3/n-Si) (Metal Insulating Semiconductor).Dielectrics are basically insulators. But, the insulators are passive materials while many dielectrics in use are active and play a vital role in many electronic applications. When a dielectric is placed in an electric field, the bounded charges within the material are polarized. The dielectric loss is the amount of energy lost in a dielectric per unit time when an electric field acts on it. In high voltage applications, the importance of dielectric loss cannot be overstated. Dielectric loss generally follows similar temperature behavior as that of the dielectric constant.In the present study, the dielectric measurements were carried using HP4192A impedance analyzer. An electrically polled sample was mounted in a two terminal sample holder. The capacitance and dissipation factor (tanθ or D) were measured with variation of temperature at different constant frequencies, directly with the impedance analyzer interfaced to a computer. A Keithley 196 system DMM is used to measure temperature. The sample holder used for resistivity measurements was also used to measure dielectric data. The sample temperature was gradually increased by regulating the input power of muffle furnace using a claimer stat (0-270V, 15amp). Fig. 3 shows that the dielectric constant has high value at low frequency. It decreases sharply at (20KHz) and remains almost constant above this frequency. This result agreement with the results of Pontes et al.

The high value of dielectric constant at low frequencies is believed in the interfacial polarization of space charges, presence of a highly resistive interfacial layer or a high density distribution of interface states.

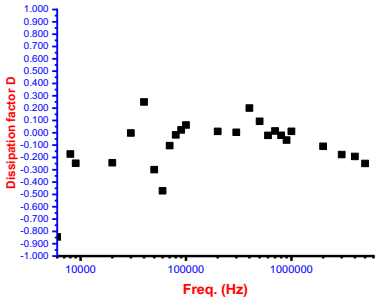

Fig. 3: The capacitance is change slightly with frequency initial.

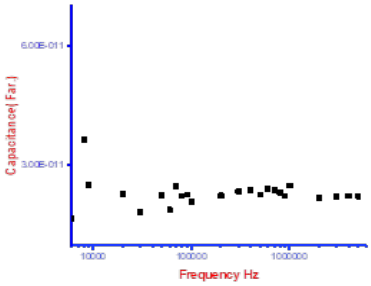

Fig. 4: dissipation factor is constant as function with frequency.

Fig. 4 shows loss factor (tan δ) variation with frequency for all prepared films at room temperature, similar behavior to that of the dielectric constant is observed.
Observe the initial level of admittance in this graph; it does not change, but after a particular frequency is reached, it begins to rise, and this trend continues with higher frequencies. After reaching a particular frequency, the imaginary component of admittance increases with increasing frequency.

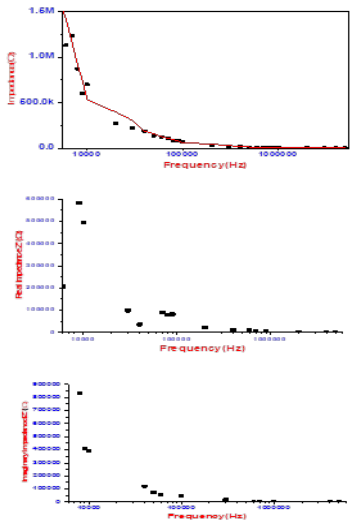

Fig. 5: The impedance is observed decreased with the increase of frequency.

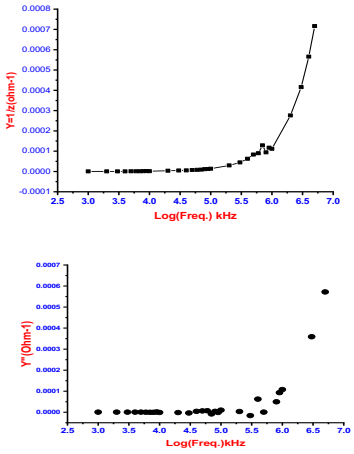

Fig. 6: Real and imaginary component of impedance increased with increasing frequency.

4.3 Hysteresis Measurement

In a poly domain ferroelectric crystal, applying a d.c. field larger than the coercive field along a polar direction aligns all Ps Vectors by moving out domain walls that separate regions with anti-parall Ps. The coercive field is measured by the minimal d.c. field necessary to move domain walls. The initial value of Ps in a poly domain crystal rises as the d.c. field is increased until it reaches the typical maximum for the material. The reversal of the field results in the reappearance of domain barriers due to the fact that it alters the way that Ps is perceived in the various regions. The crystal will have a remnant polarization that is no bigger than the spontaneous polarization when there is no applied field. The magnitude of the final is will be the same as that of the initial full is, but the sign will be the opposite when the field is in complete reverse. The work required to move domain walls determines the hysteresis, which is intimately related to the detect distribution in the crystals and the energy barrier separating the two orientation states. In the present sample the hysteresis loop observed is shown in the figure. No saturation could be observed in the present sample. The remnant polarization and coercive filed observed are smaller than those expected for SrTiO3. Only a circular loop could be observed.

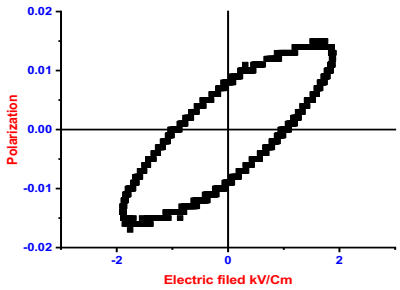

Fig. 7: Polarization vs Electric field of SrTiO3 Thin film.

Surface resistivity could be defined as the material's inherent surface resistance to current flow multiplied by that ratio of specimen surface dimensions (width of electrodes divided by the distance between electrodes) which transforms the measured resistance to that obtained if the electrodes had formed the opposite sides of a square. In other words, it is a measure of the material's surface inherent resistance to current flow Surface. Resistivity does not depend on the physical dimensions of the material. The resistance of a square sample could be considered by analogy with an electric circuit to be a resistor with resistance R_0. Fig. 8 shows variation of resistivity with temperature. Resistivity decreases with increase of temperature. Initially the resistivity decreased with the increase of temperature. In the high temperature region slope of the curve gives activation energy for intrinsic conduction.

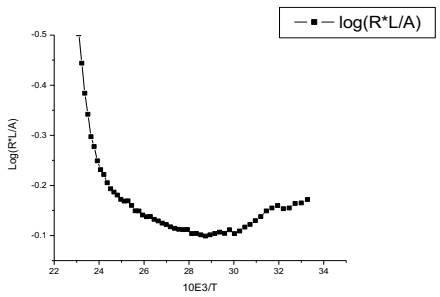

Fig. 8: variation of resistivity with temperature.

Data will not be shared because these data help study the correct choice of correct form for suitable applications.

5 Conclusions

By using rf magnetron sputtering at different substrate temperatures, thin layers of SrTiO3 (STO) were put on p-type Si(100) substrates. The thickness of the coatings varied between 300 and 500 nm, whereas the deposition temperature remained constant at 550°C. The XRD pattern for the SrTiO3 thin film reveals that it is in the cubic phase. Metal-insulator-semiconductor (Al/STO/p-Si/Al) was manufactured and characterized through capacitance-voltage, current-voltage, and admittance spectroscopy measurements. The dielectric constant decreased with increasing frequency. The impedance decreased with increasing frequency. The coercive field is measured by the minimal d.c. field necessary to move domain walls. The initial value of Ps in a poly domain crystal rises as the d.c. field is increased until it reaches the typical maximum for the material.

Acknowledgments
The authors would like to express their gratitude to everyone who assisted them in completing this study.

Conflict of Interest
The authors declare no competing financial interest; there is no funding for the project.

References

[1] E. Defaÿ, Integration of Ferroelectric and Piezoelectric Thin Films. 2011.
[2] H. A. Gatea, "Synthesis and characterization of basrti03 perovskite thin films prepared by sol gel technique," *Int. J. Thin Film Sci. Technol*., vol. **10**, no. 2, pp. 95–100, 2021
[3] S. Jiang, H. Zhang, R. Lin, S. Liu, and M. Liu, "Electrical properties of BST thin films fabricated by a modified Sol - Gel processing," *Integr. Ferroelectr*., vol. **70,** no. December 2014, pp. 1–9, 2005.
[4] H. A. Gatea, "Effect of High Temperature on Thermal Analysis, Structure and Morphology of CeO2 Nanoparticles Prepared by Hydrothermal Method," *Int. J. Thin Film Sci. Technol.*, vol. **11,** no. 2, pp. 201–206, 2022.
[5] H. A. Gatea, H. Abbas, and I. S. Naaji, "Effect of Sr+ ion Concentration on Microstructure and Dielectric properties of Barium Strontium Titanate Ceramics," *Int. J. Thin Film Sci. Technol*., vol. **11**, no. 2, pp. 239–244, 2022.
[6] N. Ortega et al., "Compositional engineering of BaTiO3/(Ba,Sr)TiO3 ferroelectric superlattices," *J. Appl. Phys*., vol. **114,** no. 10, 2013.
[7] H. A. Gatea, "Impact of particle size variance on electrical and optical properties of Ba1-xSrxTiO3," *J. Mater. Sci. Mater. Electron.*, vol. **34**, no. 6, pp. 1–12, 2023.
[8] H. A. Gatea and I. S. Naji, "The effect of Ba/Sr ratio on the Curie temperature for ferroelectric barium strontium titanate ceramics," *J. Adv. Dielectr*., vol. **10**, no. 5, pp. 1–11, 2020.
[9] I. S. Naji and H. A. Gatea, "Influence of sintering temperature on ferroelectric ba0.7sr0.3tio3 microstructure, grain size, and electrical properties," *Int. J. Thin Film Sci. Technol.,* vol.**9**, no. 2, pp. 133–141, 2020.
[10] H. A. Gatea, "Effect of Substrate-induced Strains on Ferroelectric and Dielectric Properties of Lead Zirconate Titanate Films Prepared by the Sol-gel Technique," *Nanosci. Nanotechnology-Asia,* vol. **11**, no. 3, pp. 322–329, 2020.
[11] Z. M. Y. li Omran Al-Sulttani, Mohammed Suleman Aldlemy, Musaddak M Abdul Zahra, Hamed A Gatea, Khaled Mohamed Khedher, Miklas Scholz, "Thermal effectiveness of solar collector using graphene nanostructures suspended in ethylene glycol–water mixtures," *Energy Reports,* vol. **8**, pp. 1867–1882.
[12] C. Jin and Z. Meng, "study on optical properties and their mechanism of basr1tio3 ferroelectric thin films prepared by sol-gel method," *Fourth Int. Conf. Thin Film. Phys. Appl. Junhao Chu, Pulin Liu*, vol. **4086**, pp. 658–663, 2000.
[13] H. A. Gatea, "The role of substrate temperature on the performance of humidity sensors manufactured from cerium oxide thin films," *J. Mater. Sci. Mater. Electron*., vol. **31,** no. 24, pp. 22119–22130, 2020, doi: 10.1007/s10854-020-04714-8.
[14] H. A. Gatea, I. S. Naji, and A. F. Abulameer, "Humidity sensing properties of ferroelectric compound Ba0.7Sr0.3TiO3 thin films grown by pulsed laser deposition," *Int. J. Thin Film Sci. Technol.*, vol**. 9**, no. 2, pp. 143–150, 2020.
[15] H. A. Gatea, "Evaluating the impact of substrate deposition on optical properties of perovskite barium strontium titanate (Ba 0 . 5 Sr 0 . 5 TiO 3) thin films prepared by pulsed laser," *Eur. Phys. J. D*, vol. **123,** 2022.
[16] O. A. Alawi et al., "Hydrothermal and energy analysis of flat plate solar collector using copper oxide nanomaterials with different morphologies: Economic performance," *Sustain. Energy Technol. Assessments*, vol. **49**, no. August 2021, 2022.
[17] HAMED ALWAN GATEA * and IQBAL S. NAJI, "Preparation and Characterization of Ba1-xSrx TiO3 by Sol-Gel Method HAMED," *AJ SIAN OURNAL* Chem., vol**. 31**, no. 1, pp. 186–190, 2019.
[18] J. Valasek, M. G. Cain, J. Tesař, and M. van Veghel, Springer Series in Measurement Science and Technology Characterisation of Ferroelectric Bulk Materials and Thin Films. 2014